THE STELLAR CONTENT OF GALAXY HALOS: A COMPARISON BETWEEN ΛCDM MODELS AND OBSERVATIONS OF M31

ANDREEA S. FONT[1,7], KATHRYN V. JOHNSTON[1,8], ANNETTE M. N. FERGUSON[2], JAMES S. BULLOCK[3], BRANT E. ROBERTSON[4,9,10], JASON TUMLINSON[5], PURAGRA GUHATHAKURTA[6]

Draft version February 1, 2008

ABSTRACT

Recent observations have revealed that high surface-brightness, metal-rich debris is present over large regions of the Andromeda (M31) stellar halo. We use a set of numerical models to determine whether extended metal-rich debris is expected to exist in galaxy halos formed in a hierarchical ΛCDM universe. We identify tidal debris in the simulations according to the current best surface brightness detection limits in M31 and demonstrate that bright features in the outer halo regions usually originate from single satellites, with very little contamination from other sources due to the low probability of tidal streams from two overlapping accretion events. In contrast, high-surface brightness features in the inner halo often originate from multiple progenitors. We also compare the age and metallicity distribution of the debris with the well-mixed stellar halos in which they reside. We find that high-surface brightness tidal debris is produced almost exclusively by relatively high mass progenitors ($M_* \sim 10^{7-9} M_\odot$) and thus is expected to be of moderate- to high-metallicity. Similarly, in our models the smooth inner halo is expected to be metal-rich as this region has been built up mainly from massive satellites. Our results imply that the stellar populations of substructure observed around external galaxies with current techniques should not resemble old and metal-poor dwarf spheroidal satellites, nor the underlying component of the stellar halo.

Subject headings: galaxies: abundances — galaxies: evolution — cosmology: theory

1. INTRODUCTION

One of the main goals of stellar population studies is to understand the origin of the baryonic components of galaxies. Stellar populations contain a wealth of information – kinematic, age and chemical abundance – that enables the reconstruction of star formation histories of the past and present-day galaxies. More recently, the growing interest in the topic of "near-field cosmology" (Freeman & Bland-Hawthorn 2002) has raised the question of to what extent stellar populations can be used to constrain cosmological models. In this paper we review recent stellar population data in M31 that appear to challenge hierarchical models of structure formation and compare these data with results of numerical simulations.

Galaxy halos are among the most interesting testing grounds for structure formation theories as they contain imprints from various star formation episodes, starting with those that took place in the earliest formed structures. Patterns in the stellar populations in different regions of a galaxy halo, or between different halos, or even between halos and their neighboring satellite galaxies, can be analyzed and compared with predictions of cosmological models.

The old and metal-poor halo of our Galaxy has long been the prototype for models of galaxy formation (Searle & Zinn 1978; Laird et al. 1988; Ryan & Norris 1991). Thanks to advances in instrumentational techniques over the last couple of decades it has now become possible to resolve stellar populations in halos of other galaxies within our Local Group: Andromeda (M31) – a galaxy similar in mass and luminosity to our Galaxy (Mould & Kristian 1986; Reitzel, Guhathakurta, & Gould 1998; Durrell, Harris & Pritchet 2001, 2004; Ferguson et al. 2002, 2005; Brown et al. 2003, 2006a,b, 2007; Ibata et al. 2007), and various satellite galaxies, such as the Magellanic Clouds, M33 and most of the dwarf spheroidals (Harris & Zaritsky 2001; McConacchie et al. 2006; Mighell & Rich 1996; Hurley-Keller, Mateo & Nemec 1998; Gallart et al. 1999; Harbeck et al. 2001; Dolphin 2002; Martin et al. 2006). Whereas the M31 and Milky Way halos exhibit similar stellar compositions (an underlying smooth, metal-poor component and a few metal-rich tidal structures), some local dwarf galaxies are quite different from the large halos. Some of these dwarfs have stellar populations that are on average younger and more metal-rich than the halo of our Galaxy, but overall display a great diversity in their stellar populations (Mateo 1998; Tolstoy et al. 2004; Dolphin et al. 2005).

Recently, it has also become possible to analyze the stellar populations in some of the faintest galactic substructure, namely in the tidal debris. In contrast with the variety of populations displayed by neighboring dwarf galaxies, the streams discovered so far are striking in their uniformity. Unlike the predominantly old and metal-poor populations of nearby dwarf spheroidal satellite galaxies, the streams discovered so far are predominantly metal-rich with significant intermediate age components (Ferguson et al. 2005; Brown et al. 2006b). Moreover, the debris has distinct ages and metal-

[1] Van Vleck Observatory, Wesleyan University, Middletown, CT 06459

[2] Institute for Astronomy, University of Edinburgh, Blackford Hill, Edinburgh, EH9 3HJ, UK

[3] Center for Cosmology, Department of Physics & Astronomy, University of California, Irvine, CA 92687

[4] Kavli Institute for Cosmological Physics, and Department of Astronomy and Astrophysics, University of Chicago, 933 East 56th Street, Chicago, IL 60637

[5] Yale Center for Astronomy & Astrophysics, Departments of Physics & Astronomy, Yale University, P.O. Box 208121, New Haven, CT 06520-8121

[6] UCO/Lick Observatory, Department of Astronomy & Astrophysics,University of California, Santa Cruz, CA 95064

[7] Institute for Computational Cosmology, University of Durham, Science Laboratories, South Road, Durham DH1 3LE, UK

[8] Department of Astronomy, Columbia University, Pupin Physics Laboratory, 550 West 120th Street, New York, NY 10027

[9] Enrico Fermi Institute, 5640 South Ellis Avenue, Chicago, IL 60637

[10] Spitzer Fellow

licities even in comparison with the surrounding halo in which it resides. In the Milky Way, the Sagittarius stream − the largest substructure discovered in the halo (Ibata et al. 1997; Majewski et al. 1999, 2003) − has significantly younger stars than the stellar halo and an average metallicity that is a few dex higher (Yanny et al. 2000; Ivezić et al. 2000; Martínez-Delgado et al. 2004; Bellazzini et al. 2006; Monaco et al. 2006; Belokurov et al. 2006). An even larger stream dominates the halo of M31 (Ibata et al. 2001). This so-called "giant southern stream" (GSS) has a mean metallicity of [Fe/H] = −0.5, higher by about 0.2 dex than the inner M31 halo (Ferguson et al. 2002; Guhathakurta et al. 2006), and by about 1 dex than the metal-poor M31 halo component (Chapman et al. 2006; Kalirai et al. 2006). The stream also has a larger fraction of intermediate-age stars (Brown et al. 2006a). Other pieces of debris discovered in M31 include the "NGC205 loop", the "G1 clump", the "North-East shelf", the "Northern spur" (Ferguson et al. 2002, 2005; McConacchie et al. 2004), etc. − the latest inventory done by Ibata et al. (2007) in M31 lists about a dozen or so tidal features. Detailed studies of different features in the color-magnitude diagrams in these regions suggest that the metallicities are uniform and high, [Fe/H] ∼ −0.4 (Ferguson et al. 2005; Faria et al. 2007).

Are all the data consistent with the hierarchical model for structure formation? At first sight, the diversity of stellar populations in the halos, tidal streams and surviving satellites is suggestive of a stochastic assembly. However, some of the data have been given another interpretation. For example, it has been argued that the *differences* in chemical abundances between neighboring satellites and the Milky Way halo exclude these satellites from the list of possible halo progenitor types (Venn et al. 2004). At the same time, one can use the *uniformity* of chemical abundances in M31's spheroid as an argument against the hierarchical scenario: if the halo formed from different progenitors, why is the debris so uniform in metallicity (Ferguson et al. 2005)? Other recent observations claiming to challenge the hierarchical scenario use as arguments the apparent lack of very metal-poor stars in some of the surviving dwarf galaxies but not in the stellar halo (Helmi et al. 2006), and the metal-poor component of the M31 extending up to large distances in an apparently homogeneous fashion (Ibata et al. 2007).

From the above arguments, it is clear that better theoretical expectations are needed in terms of the distribution of stellar populations in dwarf galaxies, stellar halos and in the debris. In a recent series of papers we have begun to compare the results of theoretical models with available data, using as a basis a set of simulations of stellar halos formed in a ΛCDM cosmology. We found that the observed differences in [α/Fe] abundances between the surviving satellites and the halo arise naturally in the ΛCDM framework (Robertson et al. 2005; Font et al. 2006a). We have also shown how the phase-space structure of current debris can be used to recover the merger histories of ΛCDM stellar halos (Font et al. 2006b; Johnston et al. in prep.) or identify halos whose merger histories are atypical for this cosmology (Johnston et al. in prep.).

In this paper we make a direct comparison between the stellar populations in our models and those in the halo of M31, down to a level of surface brightness similar to current detection limits. We choose M31 because this galaxy has benefited in recent years from a systematic study of its stellar populations, using either deep HST photometry, deep field spectroscopy or dedicated wide-field surveys (Ferguson et al. 2002, 2005; Brown et al. 2003, 2006a,b, 2007; Guhathakurta et al. 2005, 2006; Irwin et al. 2005; Gilbert et al. 2006, 2007; Kalirai et al. 2006; Ibata et al. 2007; Tanaka et al. 2007). As a result, some aspects of the stellar populations in the M31 halo are known better now than those in the Milky Way, where observations target mainly the Solar neighborhood. In addition, M31 exhibits a wide spread distribution of metal-rich debris throughout its halo. Our aim is to investigate whether this distribution is consistent with the hierarchical merger model. We use the age − metallicity relation (AMR) as an indicator for the formation of stars in our systems (both in the smooth stellar halo and in the tidal streams). We then compare the AMRs from our simulations with those obtained from the available stellar population data in M31.

We also seek to constrain the origin of the bright, metal-rich debris in stellar halos (and in particular in M31). In observations it is often difficult to disentangle multiple stream components in the debris. In some cases the stars may belong to overlapping orbits of a single satellite (as it is now becoming evident in the case of the Sagittarius stream in the Milky Way). In others, the "debris" could be just the perturbed or warped outer disk − as it may be the case for some of the recent detections near the edges of M31 and Milky Way's disks (Momany et al 2006; Faria et al. 2007). When available, kinematic data can be used to separate the streams in phase-space (Helmi & de Zeeuw 2000), and the modelling of orbits can further connect stellar features that are physically separate on the sky. Additionally, it is conceivable, although not yet proven, that stellar populations can be used as "tags" for the individual satellites from which they originate. In this paper, we use a statistical sample of bright tidal debris fields to provide a quantitative prediction for their origin. We estimate the average number of satellites per field with significant contributions to the bright debris, both in the inner and outer simulated halos. We also analyze the average metallicity of the bright debris and found that it is in good agreement with the observations in M31.

The paper is structured as follows: In section 2 we summarize the models. In section 3 we present the AMRs of the main galaxy halos (§3.1) and of tidal streams (§3.2). In section 3.3 we investigate the origin of the highest surface brightness features (§3.3.1), their typical ages and metallicities (§3.3.2). In Section 4 we make detailed comparisons with available M31 data, for the halo (§4.1) and the GSS (§4.2 and §4.2.2). In Section 5 we conclude.

2. MODELS

The set of stellar galaxy halos used here has been constructed by Bullock & Johnston (2005) and it comprises 11 dark matter halos of mass $M_{vir} = 1.4 \times 10^{12} M_{\odot}$ formed in a ΛCDM Universe ($\Omega_m = 0.3$, $\Omega_\Lambda = 0.7$, $h = 0.7$, and $\sigma_8 = 0.9$). For our discussion we will also refer to these as L_* galaxy halos.

Full details about the set-up of the simulations can be found in the previous papers (Bullock & Johnston 2005; Robertson et al. 2005; Font et al. 2006a). Here we just briefly summarize the main characteristics of the models. The merger history of the galaxies is based on an Extended Press-Schecter formalism (Lacey & Cole 1993) and the evolution of each satellite is followed with a numerical simulation after accretion onto the main halo. The baryonic components are modeled with semi-analytical prescriptions. The infall of cold gas into each satellite is followed from the epoch of reion-

ization to the time of its accretion onto the main halo. The gas mass is translated into a stellar mass through a simple star-formation prescription and the stellar profile is assumed to follow a King (1962) model. Star formation ceases soon after accretion onto the main halo when the gas is assumed to be lost due to ram-pressure stripping. The chemical evolution of the accreted substructure is followed with the method of Robertson et al. (2005), which takes into account the enrichment from both Type II and Type Ia supernovae and models feedback as metal-enriched winds from both supernovae and intermediate mass stars. The models evolve with redshift, but are calibrated only at redshift $z = 0$ to match the stellar mass − metallicity relation, $M_* - Z$, and the stellar mass − circular velocity relation, $M_* - v_{circ}$, for Local Group dwarfs.

When evolved to the present day, the models match the main physical properties of the two main galaxies in the Local Group and of their progenitors: the number of bright ($>$ $10^5 L_\odot$) surviving satellites per main galaxy, and the masses, density profiles and total luminosities of the stellar halos are similar to those found in the Milky Way and M31. The average metallicities of our simulated L_*-type galaxy halos range between −1.3 and −0.9. The model also retrieves the differences in the [α/Fe] abundances between stellar halos and the surviving satellites. More details about the spatial distribution of chemical abundances ([Fe/H] and [α/Fe]) in these stellar halos can be found in Font et al. (2006a,b).

3. RESULTS

3.1. *Predicted properties of stellar halos*

The AMR of a stellar population is a useful tool for gaining insight into the chemical evolution of the system. In a closed box system, it is expected that the oldest populations will be the most metal poor whereas the youngest ones the most metal rich. The slope of the AMR can vary, being generally steeper for the initial stages of the evolution. The AMR will be monotonic only for isolated systems that formed monolithically (Pagel & Patchett 1975; Binney & Merrifield 1998), while systems that formed by accretion of satellites will display a composite functional form, with multiple metallicity components for the same age. In this section we use our models to investigate to what extent the AMR of a stellar halo can be used to place constraints on the galaxy mass assembly history.

Figure 1 shows the AMR of our "typical" stellar halo, constructed by averaging over all 11 halos in our sample. Each symbol represents a cell in the 2-dimensional age − [Fe/H] grid where there are any stars[11], with the area of the symbol corresponding to the mass fraction contributed by the stellar population to the total stellar mass of the averaged halo. Only the inner 50 kpc of the stellar halos are considered for this plot.

The AMR in Figure 1 has a number of distinctive characteristics: 1) the AMR has a single dominant sequence rather than being composed of multiple ones; 2) the sequence is representative of satellites that are massive, i.e that enrich to [Fe/H] > -1 values in just a few Gyrs; and 3) the ages of the stars are typically old, > 8 Gyr. These characteristics are a direct consequence of the merger histories of inner halos assumed for our ΛCDM models, and which have been described in more detail in previous papers (Bullock & Johnston 2005; Font et al. 2006a,b). The dominant AMR sequence oc-

---

[11] We henceforth consider all stars in a given grid age − [Fe/H] cell to be a distinct stellar population.
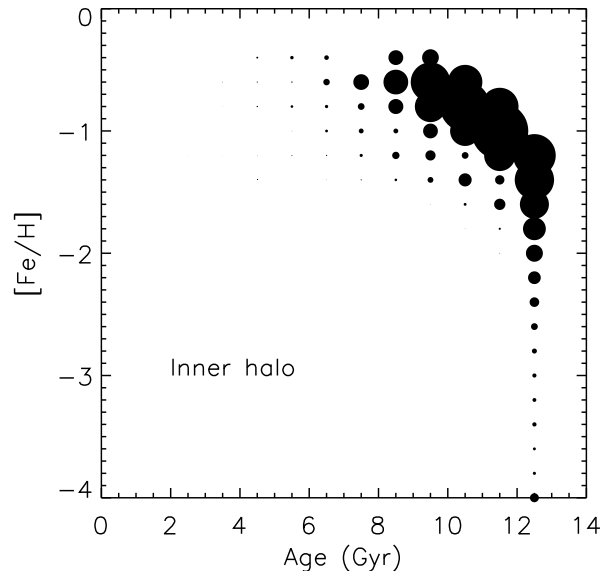

FIG. 1.— AMR for the average of all 11 halos in our sample. Only the inner 50 kpc regions of the halos have been considered here. The area of symbols varies with the mass fraction of stellar populations to the total mass in the field. (No population contributes, by mass, more than 25% to the halo.)
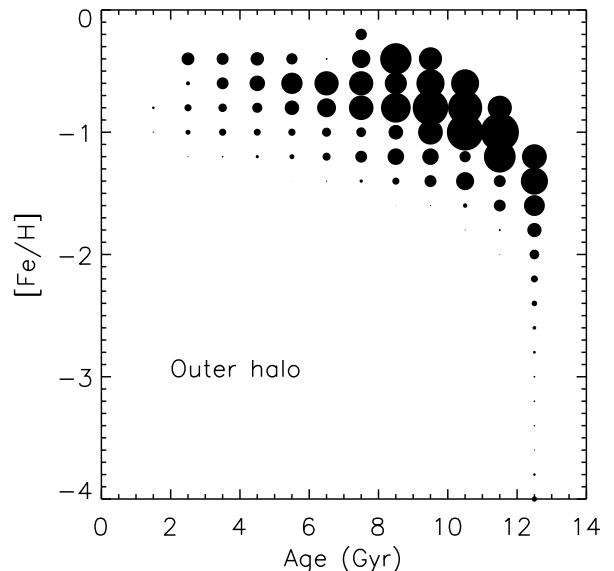

FIG. 2.— AMR for the outer region ($50 < R$ kpc) of the averaged simulated halo. Symbol areas correspond to the stellar mass fraction contributed by the population, as in Figure 1. The fraction of each population is normalized to the stellar mass of the entire outer halo region.

curs because the bulk of the inner halo is formed from a few massive satellites ($10^7 - 10^8 M_\odot$), even though the main halo accreted satellites with a broader range of stellar masses ($M_* \sim 10^4 - 10^8 M_\odot$). In addition, massive satellites sink more rapidly into the center due to a more effective drag of dynamical friction. The major contribution to the total stellar mass of massive satellites also explains the clear signature of rapid metal enrichment (more details about the AMRs of individual satellites are given below). Few stars have ages < 8 Gyrs, and
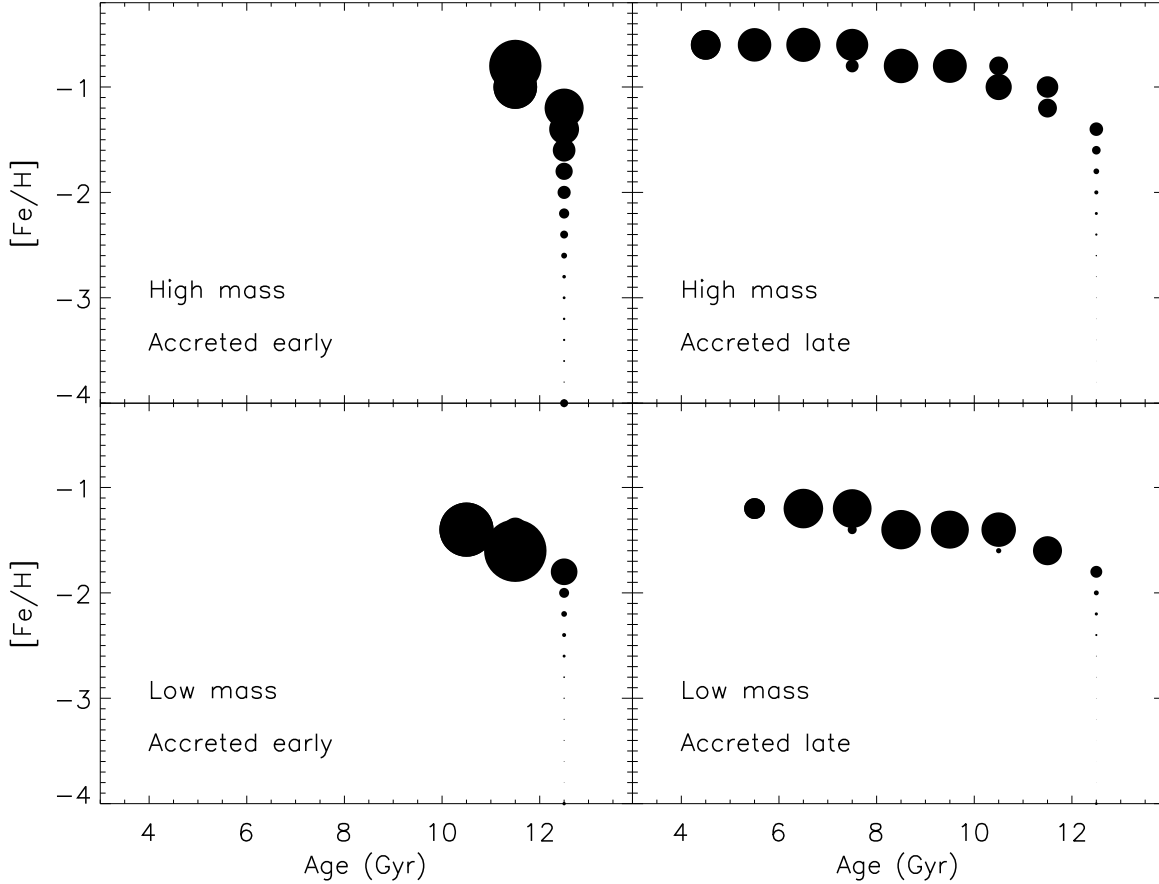
FIG. 3.— AMRs of individual satellites of various masses and accreted at different times. The low mass satellites chosen here have $M_* \sim 10^6 M_\odot$, while the high mass ones have M_* of a few $10^8 M_\odot$. The accretion times are of $1-2$ Gyr for the early events and $6-7$ Gyr for the late ones. Symbol areas correspond to the stellar fraction contributed by the population, as in Figure 1. The stellar mass fractions are normalized to the total stellar mass of each satellite.

this is because early events dominate the inner halo accretion history.

Spatial variations in the stellar populations properties across hierarchically-formed halo are also of observational interest. Figure 2 shows the AMR of the outer regions of halos ($R > 50$ kpc), using the stellar population data of the same averaged halo as in Figure 1.

The larger spread in ages in the outer halo is a consequence of the late assembly of this region compared with the inner one (Bullock & Johnston 2005; Font et al. 2006a). Given the evolution with time of the typical mass of the accreted systems, the outer halo is formed from satellites with higher masses, $M_* \sim 10^6 - 10^9 M_\odot$, than the inner halo. Of note, is the presence of very massive satellites in the outer halo, $M_* \sim 10^9 M_\odot$, which extend the outer halo AMR towards $[Fe/H] \sim 0$ values.

Our results indicate that an averaged sample of the outer halo should display a significantly larger fraction of intermediate-age versus old stars than the inner halo. The metallicity distribution function should also have a broader peak in the outer halo.

3.2. *Predicted properties of individual satellites and streams*

By construction our simulated satellites have a monotonic chemical enrichment. This limitation results from a number of simplifying assumptions − for example, the merger history of a satellite is approximated with a general formula

(Wechsler et al. 2002) and not followed stochastically, and the gas and metals are assumed to be instantaneously mixed after each star formation episode. The predictive power of our models for individual satellites (and streams) is therefore restricted. The individual AMRs will underestimate the scatter in [Fe/H] for stellar populations of the same age. However our models are fairly reliable in matching the mean metallicity of satellites and the overall AMR sequence.

Figure 3 shows four cases of individual satellites in the range of stellar masses and accretion times that are typically found in our simulations. Despite the limitations in modelling the entire scatter, some trends are obvious. For example, satellites have a smaller [Fe/H] spread at a fixed age than the outer halo but the spread is comparable to that of the inner halo. Also, the overall shape and maximum [Fe/H] of the inner halo AMR are similar to those of massive satellites ($M_* > 10^8 M_\odot$).

The AMR of the outer halo contains individual AMR sequences that are more clearly separated (Figure 2) than those in the inner region of the halo (Figure 1). As each AMR sequence corresponds to a single satellite or a group of satellites with similar properties, this suggests that using AMRs as a tool to disentangle the accretion histories of stellar halos may be more feasible in the outer rather than in the inner regions of the halos.

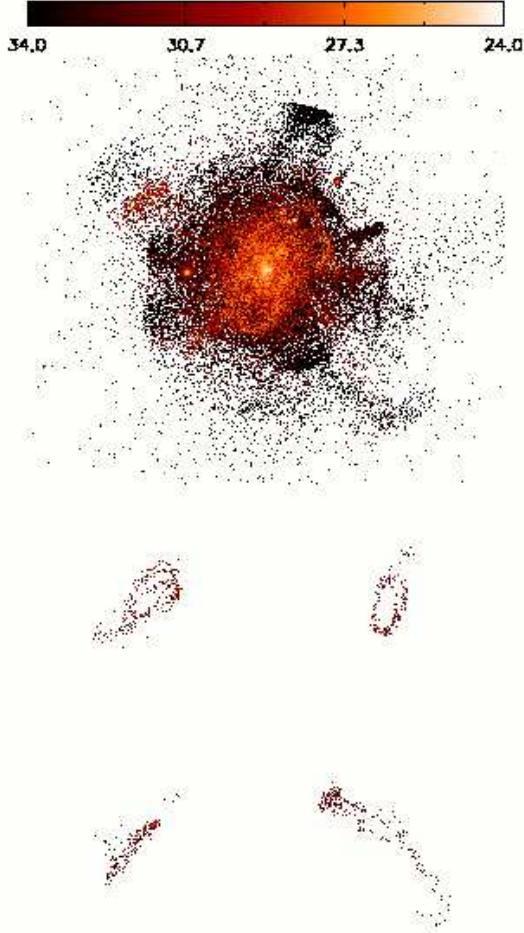### 3.3. *The Extended, High Surface Brightness Debris*

FIG. 4.— *Top:* A stellar halo mapped in surface brightness down to 34 mag/arcsec^2(this is halo H2 in Font et al. (2006b)). The region shown here extends 150 kpc on the side. *Middle and bottom:* Four examples of kinematically cold streams surviving at present time in the halo above. The streams have been shrunk to a quarter of their size, for illustration purposes.

3.3.1. *Origin*

What is the origin of the bright, metal-rich debris extending over large areas in the M31 halo? Was a single satellite responsible for polluting the M31 halo with metal-rich stars or were they several? Here we use our models to constrain the formation history of this debris, assuming that it formed entirely from merging events.

The upper panel in Figure 4 shows the surface brightness map of a stellar halo with M31-like properties. The map shows only the surface brightness down to the limit of $\mu_V = 34$ mag/arcsec^2, which is roughly the deepest limit achieved currently by wide field surveys of the M31 (Ferguson et al. 2002; Irwin et al. 2005; Ibata et al. 2007). The bottom panels in Figure 4 show the surface brightness maps of the main four kinematically cold streams surviving at the present time in the simulated halo.

Down to the chosen surface brightness cut, the spatial distribution of the simulated debris is similar to what has been found so far in M31 and in the Milky Way: there are a few bright kinematically cold streams (the counterparts of the Sagittarius stream, the GSS or the NGC205 loop), the rest of the debris being in the form of much fainter streams or diffuse overdensities.
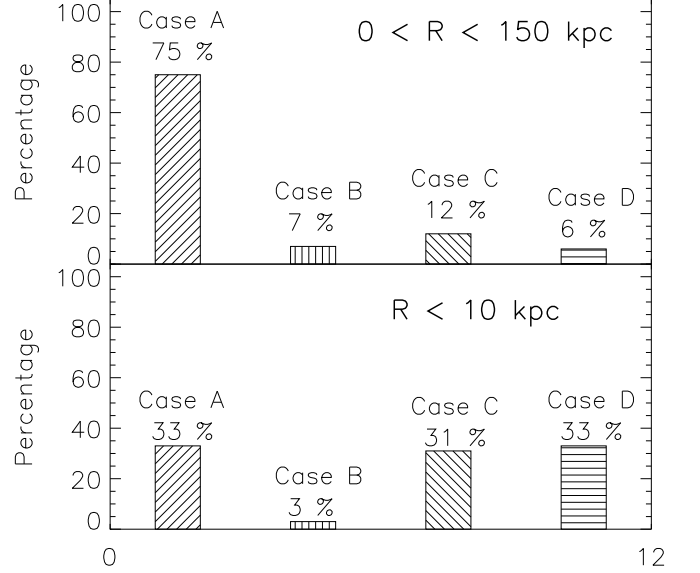

FIG. 5.— The origin of high surface brightness fields ($\mu_V \leq 30$ mag/arcsec^2): a single source (case A), two dominant sources (case B), multiple less dominant sources (case C) and diffuse material originating in many minor sources (case D). *Top panel:* All bright fields across the halo are selected; *Bottom panel:* Only the bright fields in the inner $R < 10$ kpc of the halo are selected.

We define as "high surface brightness" all debris that is as bright (or brighter) than the current detections of substructure $- \mu_V \sim 30$ mag/arcsec^2 for the GSS in M31 (Ibata et al. 2001). We therefore select for our analysis all fields which have $\mu_V \leq 30$ mag/arcsec^2 and that are located on the projected area of a halo along the line of sight. These mock fields have the same area as the pixel size area of the halo map in Figure 4, i.e. 0.4×0.4 kpc. The depth of the field along the line of sight is of the same order as the virial radius of the main galaxy, i.e. $\simeq 300$ kpc. The total surface brightness in each pixel is obtained by integrating over all populations in the field.

We then divide all bright fields into four disjoint cases, based on the formation history of the stellar overdensity in that field:

- case A: The overdensity originates mainly in a single satellite. The condition we impose is that the satellite contributes a mass fraction $f > 80\%$ of the total stellar mass in the field;
- case B: The overdensity is formed from contributions of two main satellites. The condition is that these satellites combined contribute more than 80% of the stellar mass in the field;
- case C: The overdensity is formed from one or more satellites with less significant contribution(s). Specifically, we require that there is at least one satellite contributing $30\% < f < 40\%$, but no satellite contributes more than 40% to the total stellar mass in the field;
- case D: The overdensity is formed from a multitude of minor satellite contributions. No satellite is contributing more than 30% of the total mass in the field.

The top panel of Figure 5 shows the frequency of each case among the bright fields over the entire area of the stellar halo. Cases in which the overdensity originates in a single satellite

(A) occur about 70% of the time, while cases B, C and D occur less frequently, each at about 10% of the time. The actual percentages vary slightly from halo to halo and depend on the imposed surface brightness limit – for example, the frequency of case A increases if we select an even brighter debris. However, case A consistently dominates across the halos. The distribution of these cases begins to reverse in the inner regions of the halos, where phase-mixing is more important. The bottom panel in Figure 5 shows the same information as the top panel, but for the inner 10 kpc of the halo. Here, the dominating cases are those in which the debris originates in three or more satellites.

These results have a number of implications for the interpretation of high surface brightness overdensities in galaxies. For example, if the overdensity is relatively distant from the center of the halo, $R > 10 - 20$ kpc, it is likely to originate in a single satellite, with little contamination from other satellites in the field. This result holds regardless of whether the feature is kinematically cold or if it is diffused in phase-space. For the inner halo, only a third of the bright features are created by a single satellite, the majority of them originating from superposition of streams from three or more satellites (cases C and D).

3.3.2. *Metallicity*

The existence of the metallicity - luminosity relation (Garnett & Shields 1987; Skillman, Kennicutt, & Hodge 1989; Brodie & Huchra 1991; Zaritsky, Kennicutt, & Huchra 1994) and the corresponding metallicity - mass relation (Lequeux et al. 1979; Tremonti et al. 2004; Erb et al. 2006) for galaxies indicates a connection between the nature of the satellite progenitors and their metallicities. We might expect a corresponding connection to exist between the surface brightness of the current debris and its overall metallicity. Given this expectation, it is useful to examine whether high surface brightness debris in our models (as analogue of the M31 observations) indeed originates in satellites of a typical stellar mass, and if so, what is the predicted average metallicity of the debris.

In our models, satellites relatively massive, $M_* \sim 10^{7-8} M_\odot$, and accreted $10 - 12$ Gyr ago result in sufficiently bright debris to be detected, $\mu_V \sim 30 - 32$ mag/arcsec^2 (Johnston et al. in prep.). As the surface brightness of the debris depends on both the mass of the progenitor, and on the time of accretion, satellites with $M_* \sim 10^{7-8} M_\odot$ accreted less than 10 Gyr ago are much brighter, $\mu_V \sim 28 - 30$ mag/arcsec^2. Satellites with stellar masses greater than $10^8 M_\odot$ assembly later and are therefore accreted later (< 8 Gyr ago), resulting in debris with the highest surface brightness, $\mu_V \sim 26 - 28$ mag/arcsec^2 (Johnston et al. in prep.). Therefore, the average metallicities of high surface brightness fields originating from a single satellite are expected to range between -1.4 and 0 (which are average values for satellites with stellar masses of 10^7 and $10^9 M_\odot$, respectively; values are quoted at the time of accretion).

A high surface brightness in a given field can be achieved not only from the contribution of a single relatively massive satellite, but also from the superposition of debris originating in several massive satellites (eg. if 80% of field stars originating in a $10^{7-8} M_\odot$ satellite reach the detection limit, i.e a case A, then a combination of two 40% fractions originating in two separate $10^{7-8} M_\odot$ satellites are equally bright, i.e a case B). In the case of superposition of massive satellites, the average metallicity of the high surface brightness field is similar to the

average metallicity of the individual satellites, i.e. the fields are expected to be metal-rich.

As we will discuss below, most of the observed debris in M31 *is* metal-rich. The average [Fe/H] in the GSS is ~ -0.5 (Ferguson et al. 2002; Brown et al. 2006b) and other debris throughout the M31 halo have similarly high metallicities, [Fe/H] ~ -0.4 (Ferguson et al. 2005; Faria et al. 2007). Additionally, Gilbert et al. (2007) show that the M31 "spheroid" fields and several fields along the minor axis are consistently metal-rich, with and without the cold GSS component. The lesson learnt from our models is that the metal-rich debris currently observed in the inner halo of M31 may not have a single common progenitor, and moreover, each individual inner halo field may contain metal-rich components from multiple sources.

4. APPLICATIONS TO OBSERVATIONS

4.1. *The M31 Halo*

Brown et al. (2006a,b, 2007) have derived the star formation histories at various locations in the outskirts of M31. The resulting ages and metallicities in these fields can be compared directly to our model predictions. A concern is that some of Brown's fields lie along the minor axis of M31, a region that has been shown to contain stars from multiple sources, including the disk and GSS (Ibata et al. 2007). The most recent field analyzed lies at 21 kpc along the minor axis and is expected to have an insignificant contribution from thin disk stars or from the giant extended disk structure detected by Ibata et al. (2005) (for evidence against contamination from the latter component, see Gilbert et al. (2007); also, note that the extended disk component may have an accretion origin as well (Peñarrubia, McConnachie & Babul 2006)). On the other hand, the 21 kpc halo field may still be contaminated by stream debris (Gilbert et al. 2007).

We note, however, that from the point of view of hierarchical models one cannot easily differentiate between a "true" or "clean" halo and a halo contaminated by debris. In this context, stellar halos are expected to form through the superposition of tidal debris and show various degrees of phase-mixing. Therefore the only concern in our comparison is not to mistake a field that is dominated by a given stream for one that is representative of the whole halo. The cautionary remark regarding our further comparison with the 21 kpc field of Brown et al. (2007) is that the presence of a cold stream in the inner halo field appears indeed to be atypical in our simulations. Whether this observed field is representative of the whole inner M31 halo, or of a typical Milky Way-type inner halo, remains to be decided by future observations.

Our strategy for further comparisons with the observations is to present averaged results rather than selected, well-matched fields. In this respect, our results do not emphasize the dispersion in stellar population data that can exist among individual halo fields. However, these differences are not expected to be as large in the inner halo as in the less phase-mixed, outer one (Font et al. 2006b).

4.1.1. *The 21 kpc Halo Field*

Figure 6 shows a comparison between the 21 kpc halo field of Brown et al. (2007) and our averaged inner halo region (bottom and top left panels, respectively). In the right panels we also show the AMR of two individual halos from our sample that have mass accretion histories that bracket the averaged one (halo H7 has a protracted mass accretion history,
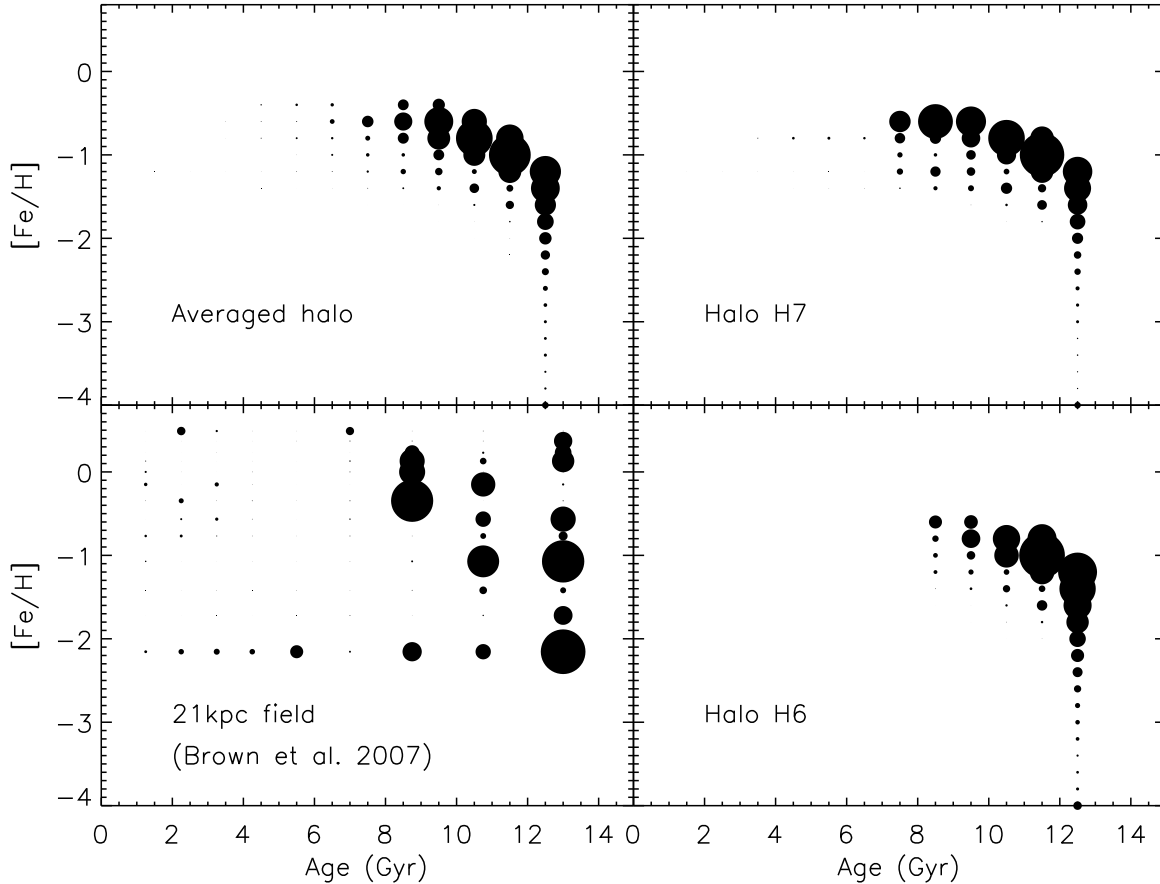
FIG. 6.— Comparison between the halo field of Brown et al. (2007) and simulated inner halo fields. Top left panel shows the averaged halo; top and bottom right panels show two individual halos with a protracted and short and mass accretion histories, respectively. Bottom left panel shows the observational data (Courtesy of Tom Brown). The symbol size in the simulated fields are as indicated in Figures 1 and 2. For the observational data, the area of the circles is proportional to the number of stars in each isochrone group (see Brown et al. (2007)).

whereas halo H6 has a short one. Halo H7 is also ~ 0.5 dex more metal-rich than halo H6).

The dominant presence of old stars in both observations and simulations is not surprising, as inner halos are expected to form within the first few Gyr from the assembly history (Bullock & Johnston 2005). The existence of intermediate-age stars in the inner halos is a new finding that can provide important constraints on the models of halo formation. Brown et al. (2006b) estimate that $\sim 40\%$ of the stars in the field 11 kpc along the minor axis in M31 are less than 10 Gyr old, while the mean age in that field is 9.7 Gyr. Brown et al. (2007) find that the field at 21 kpc along the minor axis has significantly less stars with ages less than 10 Gyr (the fraction is about half of that in the inner field), and virtually no stars with ages less than 8 Gyr. The distribution of populations in the latter field seems to be more into agreement with our models, which predict that about 20% of populations in the inner halo have ages less than 10 Gyr.

The AMRs of the simulated halos show non-negligible populations with intermediate metallicities $-2 <$[Fe/H]< -1 and ages younger than $10-11$ Gyr. Although these populations represent only a minor contribution ($< 1\%$, by mass) to the entire stellar halo, they can provide important information about the halo formation history. In our models, stars with these ages and metallicities predominantly come from lower-mass, metal-poor halo progenitors, and hence are a probe of

the accretion of dwarf galaxies at the lower end of the mass function. (Note: the lower metallicity of low mass halos follows because we imposed that dwarfs accreted today follow the $M_* - Z$ relation (Dekel & Silk 1986; Dekel & Woo 2003).)

The old and metal-poor stars with ages > 10 Gyr and [Fe/H] < -2, located in the lower right corners of the AMRs, are good tracers of the early stages of star formation in galaxy halos or in their progenitors. Both our models and the observations show non-negligible fractions of such metal-poor stars (note: the Brown et al. (2007) AMR shows only stars with [Fe/H] > -2, but this may only be an artifact of the limited choice of metallicities in the isochrone dataset). At the moment there is a great interest in finding the most metal-poor stars in halos of galaxies and in understanding their origin. Apart from the evidence that the M31 halo has some very metal-poor stars (Brown et al. 2004, 2006b, 2007), the searches also target the Milky Way halo (Beers & Christlieb 2005). In our models most of the stellar populations form in small sub-halos at high redshift and enter the main halo in relatively massive satellites. Improved models that track the early episodes of star formation and metal enrichment in more detail will be able to provide better constraints on the origin of this type of populations (see Tumlinson et al, in prep.).

Interestingly, the observed AMR of Brown et al. (2007) contains some stars that are more metal-rich than the stars of the same age in our simulated halos (see, in particular, the

[8 Gyr,12 Gyr] age interval). This rapid enrichment is indicative of stars originating in a fairly massive satellite, of $\sim 10^9$ or a few $10^8 M_\odot$ in stellar mass (see, for example the AMRs of massive satellites in Figure 3). The reason that our simulated halos do not show such signatures is that most of the progenitors of these well-mixed regions have stellar masses of $10^{7-8} M_\odot$ or less. According to our models, the accretion of a $M_* \sim 10^{8-9} M_\odot$ satellite is a rare event it it were to occur more than 8 Gyr ago. A more recent accretion of such a massive satellite is possible, however the chances that the satellite is fully disrupted such that it mixes with the rest of the halo are small, unless its orbit is extremely radial. A possible explanation for the origin of these old and metal-rich populations is that they originate in the GSS (recall that the 21 kpc field of Brown et al. (2007) *is* contaminated by the GSS; and that the progenitor of the GSS is believed to have been fairly massive and on a radial orbit. See also the discussion of the GSS data in sections §4.2.1 and §4.2.2).

There are also a number of discrepancies between our models and the observations of Brown et al. (2007). The stars with ages < 5 Gyr and [Fe/H] > −1 in the top left corner of the observed AMR cannot be matched by our models. It is, however, unlikely that these extremely young and metal-rich stars belong to the halo. We hypothesize that they are either caused by a very minor contamination by the disk in this field, or that they belong to a recently accreted stream. The reason that our simulated AMRs do not have this young and metal-rich component is because, *on average*, streams of satellites accreted less than 6 Gyr ago are not found in this inner regions of our simulated halos.

Other more extreme types of populations inferred by Brown et al. (2006b, 2007) in the halo of M31 are also not easily retrieved in our models – for example, the trace populations of young and extremely metal-poor stars (ages < 10 Gyr and [Fe/H] < −2) in the bottom left corner of the observed AMR or the old and metal rich stars (ages > 10 Gyr and [Fe/H] > −0.5) in the top right corner of the same diagram. The reason for this mismatch may be that the modelling of the gas and stellar physics in our models is too simplistic to account for these populations. However it is difficult to understand what type of satellite systems would have such unusual paths of chemical evolution. In particular, if the young stars with metallicities [Fe/H] < −2 do indeed have a merger origin, it implies that the progenitor satellites either formed only recently and in relative pristine environments, or that the mixing of metals inside these satellites was very inefficient. We note, however, that while the presence of these extreme populations was derived from the Brown et al. (2006b) analysis, the authors note themselves that they may not actually be required. Indeed, Brown et al. (2006b) showed that old metal rich stars could easily be excluded from their model without diminishing the goodness of fit. Furthermore, they point out that what appears as a young metal poor population in their CMD could at least partially be explained as a population of blue stragglers.

4.1.2. *The Outer Halo*

Figure 2 also shows that the metal-poor populations ([Fe/H] < −2) extend out to large distances in the halo, in agreement with recent observations in M31 which detect an underlying metal-poor halo component out to ~ 150 kpc (Chapman et al. 2006; Gilbert et al. 2006; Kalirai et al. 2006; Ibata et al. 2007).

We find that the ratio of metal-poor stars to metal-rich stars

is higher in the outer halo than in the inner one[12]. This result appears to be in agreement with observations that find that the overall metallicity of stars decreases with radius in the M31's spheroid (Bellazzini et al. 2003; Kalirai et al. 2006; Brown et al. 2007). In contrast, the density profiles derived by Irwin et al. (2005); Ibata et al. (2007) for the metal-poor and metal-rich populations in M31 appear very similar, suggesting that the ratio of these populations is fairly constant from inner to the outer halo.

We also predict that the outer regions of the halos should have, on average, younger ages than the inner ones, as a consequence of the inside-out growth of these halos. The two fields examined by Brown et al. (2007) at 11 kpc and 21 kpc along the minor axis of M31 show an inverse trend. However, it is likely that the excess of younger stars detected in their inner field is the result of contamination by the disk, rather than a genuine trend (however, note that Brown and collaborators argue against disk contamination in the 11 kpc field). It is certainly desirable to have a detailed analysis of *both* ages and metallicities in more fields across the M31 halo before drawing a definitive conclusion about the age and metallicity gradients in this system.

4.2. *The Giant Southern Stream*

4.2.1. *Stellar Populations*

Figure 7 shows the AMR of the GSS field derived by Brown et al. (2006b) alongside the AMRs of several simulated streams. We have chosen for this comparison only streams that have massive progenitors, $M_* > 10^8 M_\odot$, as several observational and theoretical studies indicate that this is the case of the GSS progenitor (Ibata et al. 2004; Brown et al. 2006a; Font et al. 2006c). For example, we find that only progenitors with total stellar masses greater than $\sim 5 \cdot 10^8 M_\odot$ are able to match the most metal-rich portion of the observed AMR. Among these massive satellites, we find that those accreted $\sim 6-7$ Gyr ago provide a better fit to the observed AMR (eg. the bottom left panel in Figure 7) and also result in tidal debris of comparable surface brightness as the GSS, $\mu_V \sim 30$ mag/arcsec^2 (Ibata et al. 2001). (A more detailed discussion about constraining the time of accretion will be given in §4.2.2).

The AMRs of satellites accreted $6-7$ Gyr ago also have about 70% of their stars younger than 10 Gyr, in agreement with what has been found in the GSS (Brown et al. 2006b).

Not all stellar population data can be matched by our models. The metal-poor populations ([Fe/H] < −2) are not as significant in the simulated AMR than in the stream field of Brown et al. (2006b). Also, as in the case of main halos, the most extreme populations detected in the GSS field, such as the top right, top left and bottom left corners of the age − [Fe/H] grid of Brown et al. (2006b) are inconsistent with our chemical evolution models.

As discussed before, the mismatch between the observations and the models can be attributed, in part, to the limitations of our current modelling of individual streams. Additionally, the observational data in the GSS field may contain stars from other components, such as the disk, other tidal debris, or the background halo. For instance, Brown et al. (2006b) estimate that about 25% of the stars in the stream

---

[12] This result does not imply that the *absolute* number of metal-poor stars in outer halo should be higher than in the inner halo. The density of metal-poor stars is expected to decrease with distance from the center of the galaxy (see Font et al. (2006b)).
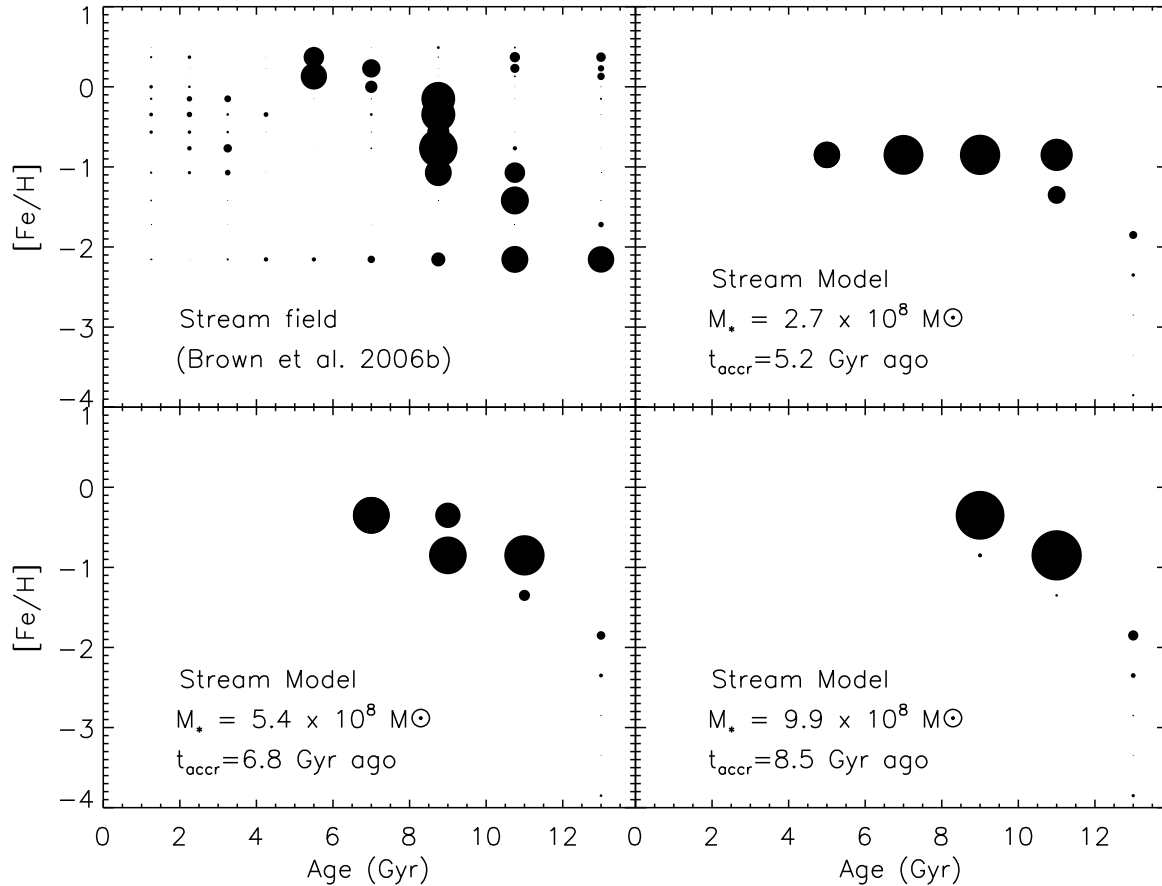
FIG. 7.— Comparison between the GSS field of Brown et al. (2006b) and several simulated streams. (Observational data are courtesy of Tom Brown). The symbol size in the simulated streams are as indicated in Figures 3. For the observational data, the area of the circles is proportional to the number of stars in each isochrone group (see Brown et al. (2006b)).

field could belong to the underlying halo. In addition, as previously discussed in §4.1.1, some of these extreme populations, such as the old and metal-rich ones, are not necessarily required for a good fit to the observations (although the young and metal-poor ones seem to be required).

4.2.2. Constraining the Time of Accretion

Although the constraints on the mass of the GSS progenitor are fairly good, the time of accretion is largely uncertain[13]. Here we discuss the possibility of putting some constraints on the latter by using our star formation history models.

Even though stellar population data contain direct information only about the star formation history of the progenitor galaxy, indirectly, they can also provide some constraints on the external mechanisms that can shut off the star formation. The accretion of the satellite onto the main halo is such a mechanism that may affect the star formation process within the satellite, slowing it down or stopping it completely. Brown et al. (2006b) suggested that the cessation of star formation in the GSS ∼ 6−7 Gyr ago might have coincided with the accretion of the progenitor satellite onto the M31. For example, if the satellite were accreted earlier than 7 Gyr ago, ram-pressure stripping along this highly eccentric orbit could have removed the gas reservoir and therefore stopped the star

formation earlier than it is observed. Similarly, if the satellite were accreted more recently, star formation would have continued several Gyrs after what is observed, unless some intrinsic mechanism would have stopped it before the accretion.

However, a time of accretion of 6−7 Gyr ago is at odds with current numerical modelling of the satellite orbit that fits the kinematic data. The simulations find that the progenitor satellite has spent less than 1 Gyr orbiting from the farthest location along the stream until the current pericenter (Ibata et al. 2004; Fardal et al. 2006; Font et al. 2006c; Geehan et al. 2006; Fardal et al. 2007), and assuming that farthest edge of the stream is the point where the satellite was accreted, it implies that the satellite must have been accreted within the last ∼ 1 Gyr.

Although the stellar population data cannot provide stringent constraints on the dynamical evolution of the satellite, the arguments above point towards a possible conflict with the numerical estimates. We examine below two possibilities: first, that the progenitor was accreted recently (< 1−2 Gyr ago), but the star formation stopped several Gyr prior to that; and second, that the satellite was accreted 6−7 Gyr.

In the first case, the question is how likely is that star formation stops several Gyrs prior to the accretion, particularly in a fairly massive satellite as it is inferred to be the case for the progenitor of the GSS. In Figure 8 we investigate this scenario quantitatively, by selecting all satellites accreted less

---

[13] The time of accretion is defined here as the time when the satellite enters the virial radius of the host galaxy.
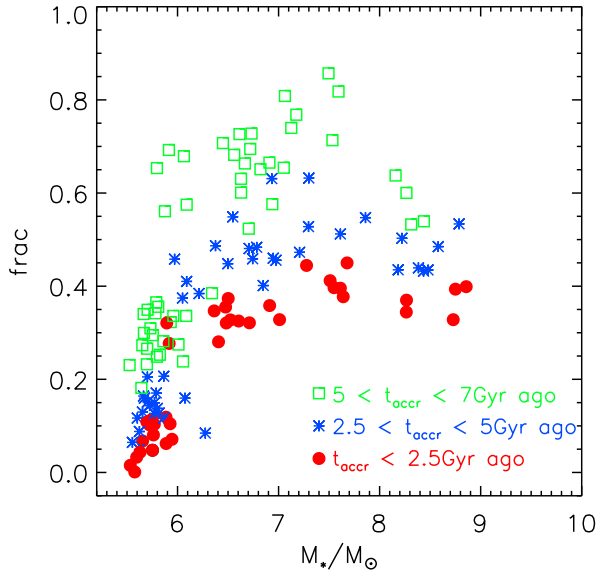
FIG. 8.— The fraction of stars formed in the 4 Gyr before the time of accretion in simulated satellites, function of the total stellar mass of the satellite. Different symbols represent different accretion times: less than 2.5 Gyr ago (red circles), between 2.5 and 5 Gyr (blue star symbols), and between 5 and 7 Gyr ago (green squares).

than 7 Gyr ago and plotting the fraction of stars formed in the 4 Gyr time interval before accretion. The satellites are divided in three categories depending on their time of accretion: satellites accreted about $5-7$ Gyr ago, satellites accreted recently (< 2.5 Gyr), and satellites accreted at intermediate times. The fraction of stars is expressed function of the total stellar mass of the satellite at the time of accretion. For more massive satellites, $M_* > 10^7 M_\odot$, – as it is assumed for the progenitor of the GSS – at least 40% of all their stars are formed within the 4 Gyr before accretion. The implication is that, if the progenitor were indeed accreted within the last $1-2$ Gyr, the observations should detect a $\sim 40\%$ fraction of young stars (ages < 6 Gyr). Current observations, however, do not detect such a high fraction of young stars (Brown et al. 2006b).

Therefore, the results based on our models seem to concur that, for a massive satellite, a time of accretion of $1-2$ Gyr ago is difficult to reconcile with a cessation of star formation 4 Gyr prior to that. The caveat, of course, is that the star formation prescription in our models may be too simplistic. The alternative is that the progenitor of the GSS was indeed accreted $6-7$ Gyr ago. In this case, it is likely that the satellite orbited more than once in the M31 halo, as the time taken to complete an orbit with the current kinematic properties is much less than $6-7$ Gyr (see the numerical simulations of Ibata et al. (2004); Fardal et al. (2006); Font et al. (2006c); Geehan et al. (2006); Fardal et al. (2007)). Also, it is also unlikely that a tidal stream that detached 7 Gyr ago would still survive today as a coherent feature. Therefore, if the satellite was accreted $6-7$ Gyr ago, the stars in the current stream must have been tidally stripped from the parent halo relatively recently. It is possible that a resolution between the results of numerical modelling and stellar population data can be achieved if the starting point of simulations is moved beyond the edge of the currently detected stream. Extrapolating the numerical

parameter space in regions which are not constrained by the data would be difficult, but certainly worth doing. The task of constraining the orbital parameters could be greatly eased if future observations find a continuation of the stream beyond the current edge, either along this orbit or on a previous one.

Our current simulations can provide some predictions on how faint the streams of satellites that undergo multiple orbits should be. The small panels at the bottom of the Figure 4 illustrate the surface brightness of a few streams formed when the parent satellite is at its first and then second passage inside the main halo. The streams are brightest when they just form, then faint with time. Therefore the streams that formed in a recent passage of a satellite inside the main halo are expected to be brighter than the streams that survive from previous a orbit of that satellite (however, the effect is attenuated by the fact that more stellar material is stripped at earlier passages of the satellite, therefore the *initial* surface brightness of the streams is higher for the streams formed earlier). We find that while the brighter (i.e. more recently detached) streams have an average surface brightness of $\sim 25-26$ mag/arcsec^2, the fainter counterparts have, on average, $\mu_V \sim 26-27$ mag/arcsec^2. These surface brightness levels should be achievable with current detection limits.

5. CONCLUSIONS

In this paper we used a set of simulations of stellar halos of L_* galaxies to study the composition of their stellar populations and provide comparisons with the observations. The test case for our comparisons was M31, given the wealth of data that exists for this galaxy. However, we emphasize that the theoretical results derived here are applicable to any large $\sim L_*$ galaxy and therefore provide a framework for interpreting the substructure of such galaxies that will be uncovered in upcoming surveys.

The main conclusions of our study are as following:

- The global stellar populations of halos assembled hierarchically will vary according to their different accretion histories. For example, the presence of metal-rich debris in a galaxy like M31 suggests a history that included the accretion of at least one massive satellite. Conversely, the more metal poor halo of the Milky Way is evidence that its progenitor satellites were less massive than those of M31.

- The homogeneous high metallicity in the inner M31 halo found by Brown et al. (2007) can be naturally explained in the context of hierarchical merging. According to our models the homogeneity of stellar populations occurs because the inner halo is dominated by a few massive satellites, $M_* \simeq 10^{7-8} M_\odot$, which had very similar star formation and chemical evolution histories. The predicted imprint of these satellites in the inner stellar halo is the presence of old stars with [Fe/H] $\simeq -1 \div 0$.

- The outer halos in our models tend to have a larger spread in the ages and metallicities of stellar populations than the inner parts. This diversity may not be apparent in current observations because the spread is contributed in part by a multitude of low-surface brightness features. Ongoing deep observations in the M31 should be able to test this prediction.

- We have investigated the origin of high surface debris in different regions of the halo. The debris in the outer $R > 10$ kpc halo typically originates in single massive satellites. This result holds regardless of whether the debris is kinematically cold or if it is diffuse in phase-space. The outer regions give the best opportunity of reconstructing the formation history of stellar halos, as their stellar populations retain information about the nature of the mergers in a non-

degenerate form.

- The origin of bright debris in the inner 10 kpc halo is more varied. Here tidal debris from a single massive progenitor or superposition of debris from several large or small satellites can result in similar surface brightness levels. Disentangling the complex formation histories of these fields is possible, provided that the interpretation of observational data takes into account the predictions of hierarchical models.

- The brightest tidal debris (i.e. that can be observed with current surface brightness limits) still orbiting around M31 or Milky Way-type galaxies should be metal-rich. Therefore it should not be expected to resemble the characteristically old and metal-poor stellar populations of dwarf spheroidal satellites, nor those of the smooth underlying halo.

- We illustrated the case of GSS in M31, whose progenitor was a massive dwarf galaxy accreted more recently than the main progenitors of the halo. The presence of intermediate-age stars and the absence of young stars suggest that the satellite could have been accreted as long ago as $6-7$ Gyr. If the satellite was accreted more than $1-2$ Gyr ago, a continuation of the stream should exist in the halo of M31, about $1-2$ mag/arcsec^2 fainter than the currently observed one.

REFERENCES

Beers, T. C. & Christlieb, N. 2005, ARA&A, 43, 531

Bellazzini, M., Cacciari, C., Federici, L., Fusi Pecci, F., Rich, M. 2003, A&A, 405, 867

Bellazzini, M., Newberg, H. J., Correnti, M., Ferraro, F. R., Monaco, L. 2006, A&A, 457, L21

Belokurov, V. et al. 2006, ApJL, 642, L137

Binney, J., & Merrifield, M. 1998, Galactic Astronomy (Princeton: Princeton U. Press)

Brodie, J. P. & Huchra, J. P. 1991, ApJ, 379, 157

Brown, T. M. et al. 2003, ApJL, 592, 17L

Brown, T. M. et al. 2004, AJ, 127, 2738

Brown, T. M. et al. 2006a, ApJL, 636, 89L

Brown, T. M. et al. 2006b, ApJ, 652, 323

Brown, T. M. et al. 2007, ApJL, 658, L95

Bullock, J. S. & Johnston, K. V., 2005, ApJ, 635, 931

Chapman, S. et al. 2006, ApJ, 653, 255

Dekel, A. & Silk, J. 1986, ApJ, 303, 39

Dekel, A. & Woo, J. 2003, MNRAS, 344, 1131

Dolphin, A. E., 2002, MNRAS, 332, 91

Dolphin, A. E., Weisz, D. R., Skillman, E. D., & Holtzman, J. A. 2005, in "Resolved Stellar Populations", eds. D. Valls-Gabaud & M. Chavez, ASPCS

Durrell, P. R., Harris, W. E., Pritchet, C. J., 2001, AJ, 121, 2557

Durrell, P. R., Harris, W. E., Pritchet, C. J., 2004, AJ, 128, 260

Erb, D. K. et al. 2006, ApJ, 644, 813

Fardal, M. A., Babul, A., Geehan, J. J., Guhathakurta, P., 2006, MNRAS, 366, 1012

Fardal, M. A., Guhathakurta, P., Babul, A., & McConnachie, A. W. 2007, MNRAS, 380, 15

Faria, D. et al. 2007, AJ, 133, 1275

Ferguson, A. M. N., Irwin, M. J., Ibata, R. A., Lewis, G. F. & Tanvir, N. R. 2002, AJ, 124, 1452

Ferguson, A. M. N. et al. 2005, ApJL, 622, L109

Font, A. S., Johnston, K. V., Bullock, J. S., & Robertson, B. E., 2006a, ApJ, 638, 585

Font, A. S., Johnston, K. V., Bullock, J. S., & Robertson, B. E., 2006b, ApJ, 646, 886

Font, A. S., Johnston, K. V., Guhathakurta, P., Majewski, S. R., & Rich, R. M., 2006c, AJ, 131, 1436

Freeman, K. & Bland-Hawthorn, J. 2002, ARA&A, 40, 487

Gallart, C., Freedman, W. L., Aparicio, A., Bertelli, G., & Chiosi, C. 1999, AJ, 118, 2245

Garnett, D. R. & Shields, G. A. 1987, ApJ, 317, 82

Geehan, J. J., Fardal, M. A., Babul, A., Guhathakurta, P. 2006, MNRAS, 366, 996

Gilbert, K. M., et al. 2006, ApJ, 652, 1188.

Gilbert, K. M., et al. 2007, ApJ, in press. (eprint arXiv:astro-ph/0703029 v2)

Guhathakurta, P. et al. 2005 (eprint arXiv:astro-ph/0502366)

Guhathakurta, P. et al. 2006, AJ, 131, 2497

Harbeck, D. et al. 2001, ApJ, 122, 3092

Harris, J. & Zaritsky, D. 2001, ApJS, 136, 25

Helmi, A. & de Zeeuw, P. T. 2000, MNRAS, 319, 657

Helmi, A. et al. 2006, ApJL, 2006, 651, L121

Hurley-Keller, D., Mateo, M. & Nemec, J. 1998, AJ, 115, 1840

King, I. 1962, AJ, 67, 471

Ibata, R. A., Wyse, R. F. G., Gilmore, G., Irwin, M. J., Suntzeff, N. B. 1997, AJ, 113, 634

Ibata, R. A., Irwin, M., Lewis, G., Ferguson, A. M. N., Tanvir, N. 2001, Nature, Vol. 412, Issue 6842, pp. 49-52

Ibata, R. A., Chapman, S., Ferguson, A. M. N., Irwin, M., Lewis, G. F., & McConnachie, A. 2004, MNRAS, 351, 117

Ibata, R. A., Chapman, S., Ferguson, A. M. N., Lewis, G. F., Irwin, M., & Tanvir, N. 2005, ApJ, 634, 287

Ibata, R. A., et al. 2007, submitted to ApJ, arXiv0704.1318v1

Irwin, M., Ferguson, A. M. N., Ibata, R., Lewis, G. F. & Tanvir, N. R. 2005, ApJL, 628, L105

Ivezić, Ž. et al. 2000, AJ, 120, 963

Johnston, K. V., Bullock, J. S., Sharma, S., Font, A. S., Robertson, B. & Leitner, S. N., 2007, in prep.

Kalirai, J. S. et al. 2006, ApJ, 648, 389

Kroupa, P. 2002, Science, 295, 82

Laird, J. B., Carney, B. W., Rupen, M. P., & Latham, D. W. 1988, AJ, 96, 1908

Lacey, C., & Cole, S. 1993, MNRAS, 262, 627

Lequeux, J., Rayo, J. F., Serrano, A., Peimbert, M., & Torres-Peimbert, S. 1979, A&A, 80, 155

Majewski, S. R., Siegel, M. H., Kunkel, W. E., Reid, I. N., Johnston, K. V., Thompson, I. B., Landolt, A. U., Palma, C. 1999, AJ, 118, 1709

Majewski, S. R., Skrutskie, M. F., Weinberg, M. D., Ostheimer, J. C. 2003, ApJ, 599, 1082

Martin, N. F. et al. 2006, MNRAS, 371, 1983

Martínez-Delgado, D., Gómez-Flechoso, M. A., Aparicio, A., Carrera, R., 2004, ApJ, 601, 242

Mateo, M. 1998, ARA&A, 36, 435

McConnachie, A. W. et al. 2004, MNRAS, 351, L94

McConnachie, A. W. et al. 2006, ApJL, 647, L25

Mighell, K. J. & Rich, M. 1996, AJ, 111, 777

Momany et al, 2006, A&A, 451, 515

Monaco, L. et al. 2006, A&A, in press. (eprint arXiv:astro-ph/0611070)

Mould, J. & Kristian, J. 1986, ApJ, 305, 591

Pagel, B. E. J., & Patchett, B. E. 1975, MNRAS172, 13

Peñarrubia, J. McConnachie, A. W. & Babul, A. 2006, ApJ, 650, L33

Reitzel, D. B., Guhathakurta, P., & Gould, A. 1998, AJ, 116, 707

Reitzel, D. B & Guhathakurta, P. 2002, AJ, 124, 234

Rich, R. M., Mighell, K. J., Freedman, W. L., & Neill, J. D. 1996, AJ, 111, 768

Robertson, B., Bullock, J. S., Font, A. S., Johnston, K. V. & Hernquist, L. 2005, ApJ, 632, 872

Ryan, S. G & Norris, J. E. 1991, AJ, 101, 1865

Searle, L. & Zinn, R. 1978, ApJ, 225, 357

Skillman, E. D., Kennicutt, R. C., & Hodge, P. W. 1989, ApJ, 347, 875

Tanaka, M., Chiba, M., Komiyama, Y., Iye, M., Guhathakurta, P. 2007 submitted (eprint arXiv:astro-ph/0704.3328)

Tolstoy, E. et al. 2004, ApJL, 617, L119

Tremonti, C. A. et al. 2004, ApJ, 613, 898

Venn, K. A., Irwin, M., Shetrone, M. D., Tout, C. A., Hill, V., & Tolstoy, E. 2004, AJ, 128, 1177

Wechsler, R. H., Bullock, J. S., Primack, J. R., Kravtsov, A. V., & Dekel, A. 2002, ApJ, 568, 52

Yanny, B. et al. 2000, ApJ, 540, 825

Zaritsky, D., Kennicutt, R. C., & Huchra, J. P. 1994, ApJ, 420, 87